Journal of Engineering Physics and Thermophysics, Vol. 68, No. 6, 1995

CERTAIN ASPECTS OF SHOCK-WAVE MOTION OF A MEDIUM CAUSED BY PHASE TRANSITIONS AND FAILURE

A. M. Petrenko and G. S. Romanov

UDC 534.222.2:539.2

The article presents the results of a numerical solution of the problem of explosion in silicate rock taking into account melting, polymorphic phase transition, and various kinds of brittle failure. We show that phase transition provides an effective increase in the stability of a medium to explosive effect, while cracking processes lead to the formation of a stable two-wave structure. A relationship between the destruction parameters and the structure of shock-wave elastic motion is established. We estimate the effect of phase transitions and failure on the spectrum of acoustic emission initiated by explosion.

In [1] results are presented concerning a solution of the problem of explosion in a medium undergoing phase transition, but without accounting for strength characteristics. Our investigation is concerned with the problem of the propagation of a shock wave in a medium that, along with phase transition, experiences different kinds of failure, since comparison of our results with those obtained in [1] makes it possible to estimate the validity of hydrodynamic approximation in calculations of explosion in a solid medium. However, the results obtained are of interest in their own right, beyond the scope of [1].

We present the results of numerical calculations of unsteady motion of a destructible medium having central symmetry initiated by an energy source in the form of a sphere of radius $r = 1$ m filled with a perfect gas with $\gamma = 1.25$ and density $\rho_0 = 10^2$ kg/m^3. At time $t = 0$, the internal energy in the sphere is distributed uniformly. The initial conditions of loading correspond to those used in [1]. We consider two variants of the problem, which differ by the functions that determine the pressure in the medium surrounding the source. In the first variant we use relations from [1] that represent the equations of state allowing for the quartz-stishovite phase transition. In the second variant we use the equation of state for quartz, also from [1], but without account for phase transition. In both variants, we use the model of brittle failure proposed in [2]. We assume that phase transition does not exert a direct effect on the elastic and strength characteristics of the medium. In the region of elastic deformations

$$\sum_{i=1}^{3} S_i^2 < 2/3Y^2, \tag{1}$$

where Y is the limit of elasticity, and S_i are the components of the deviator of stresses, which are connected with the components of the tensor of deformations by Hooke's law. When (1) is violated, brittle destruction occurs, and the medium is crushed and reduced to rubble. When stresses exceed the ultimate breaking strength $\sigma_r > \sigma_k$ or $\sigma_\vartheta > \sigma_k$, where σ_r and σ_ϑ are the radial and tangential stresses, cracking takes place. In that case, the internal and kinetic energies, stresses, and specific volume undergo changes in jumps. The magnitudes of these jumps are calculated from relations given in [2]; the values of σ_k and Y are also taken from that work.

The problem is solved with the help of a numerical method of continuous calculation with an artificial viscosity. The algorithm is based on the use of a fully conservative Lagrange difference scheme, given in [3], that approximates a system of partial differential equations. This system describes the motion of the medium and

Academic Scientific Complex "A. V. Luikov Heat and Mass Transfer Institute of the Academy of Sciences of Belarus," Institute of the Solid-State and Semiconductor Physics, Academy of Sciences of Belarus, Minsk. Translated from Inzhenerno-Fizicheskii Zhurnal, Vol. 68, No. 6, pp. 897-904, November-December, 1995. Original article submitted April 11, 1994.

 1062-0125/95/6806-0718$12.50

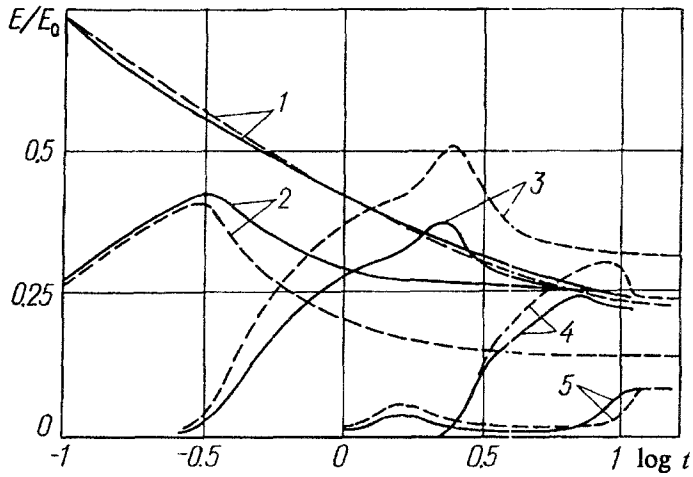

Fig. 1. Time dependences of different kinds of energy: 1) of the source; 2) of the melt; 3) of the region of fragmentation; 4) of the region of cracking; 5) elastic energy.

represents the mass, momentum, and energy conservation laws. Being indivergent, such a scheme makes it possible to judge the accuracy of computations and the quality of numerical experiments on the basis of energy balance. After the passage of 30,000 time layers, the energy disbalance amounts to 0.12% of the original energy. The calculation covers a wide range of shock-wave loading that ensures a variety of state transformations of the medium, from melting and polymorphic phase transition to different kinds of failure up to the emergence of an elastic wave.

The results of numerical calculations are presented in Figs. 1-4, where the solid lines relate to the first variant, and the dashed lines to the second. All of the quantities are given in dimensionless form, with the unit of distance being $R_0 = 1$ m, the unit of velocity $C_0 = 10^3$ m/sec, the unit of time $t_0 = R_0/C_0$, and the unit of stress $\sigma_0 = \rho_0 C_0^2$, where $\sigma_0 = 10^8$ Pa (1 kbar). Time dependences of different forms of energy are presented in Fig. 1 in units (E_0) of source energy; the trajectories of the contact boundaries, perturbation front, and elastic precursor are given in Fig. 2. From these figures it is seen that calculations gave a sequence of shock wave-induced transformations of the medium that is qualitatively consistent with physical concepts, namely, the formation of a system of concentric regions differing in their physicomechanical properties. It is seen that each of these regions, except for the region of elastic motion (see below), goes through three stages in its development. The mass and energy of the region increase in the first stage, its mass is stabilized, its energy is decreased and partially transferred to the next incipient region in the second stage, and its energy and boundary are stabilized in the third stage. Near the source, at the shock wave front (SWF), the medium experiences a quartz-stishovite phase transition, but does not experience it in the second case. Moreover, if the specific internal energy exceeds the specific energy of melting, which was assumed to be identical for the two phases and equal to $0.97 \cdot 10^3$ kJ/kg, the medium is considered a melt. Its motion is calculated in a hydrodynamic approximation. It is assumed that the stishovite does not change to quartz. In Fig. 1 curves 1 represent the energy of the source, and curves 2 pertain to the energy contained in the melt. In Fig. 2, curves 1 represent the trajectories of the source boundaries, and curves 2 pertain to the trajectories of the boundary of the melt. As the intensity of the shock-wave decreases sufficiently, the process of melting terminates; phase transition and crushing of the stishovite occur in the first case and crushing of the quartz in the second. As the wave becomes weaker, the phase transition ceases, and quartz crushing occurs in both cases at the SWF. In Fig. 2, curve 3 represents the trajectory of the phase interface, and curves 4 show the trajectories of the boundary of the fragmentation region. In Fig. 1 curves 3 pertain to the energy contained in the region of fragmentation. Initially the fragmentation occurs at the SWF, and the velocity of the front exceeds the speed of sound. Later on, as the loadings at the SWF decrease, the fragmentation-front velocity drops and becomes subsonic. And at once it starts to generate an elastic wave. As the boundary of the fragmentation region is slowed down, the energy of elastic motion increases (Fig. 1, curves 5). However, with a further decrease in loading, the mechanism of failure changes. Criterion (1) does not hold any longer, but tangential stresses exceed the ultimate

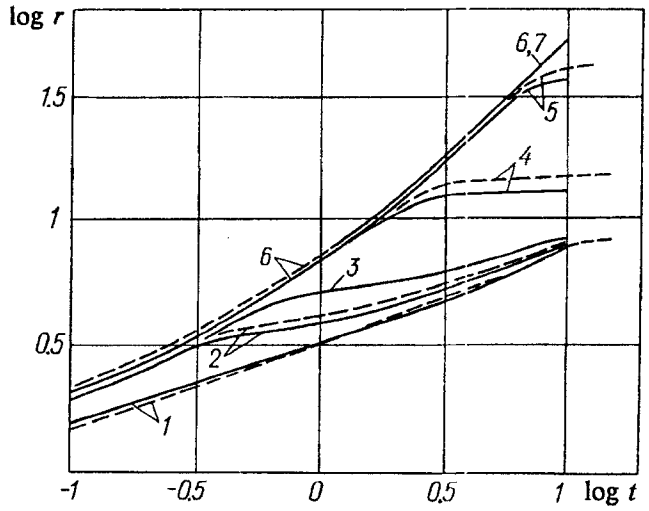

Fig. 2. Trajectories of contact boundaries and of the stress amplitudes: 1) source; 2) melt; 3) stishovite-quartz phase interface; 4) fragmentation region; 5) region of radial cracks; 6) front of basic perturbation; 7) elastic precursor.

strength: $\sigma_\vartheta > \sigma_k$. Radial cracks are formed. The magnitudes of the stresses and of the internal energy undergo changes in jumps; the kinetic energy of the medium also increases in a jumpwise fashion, leading to an increase in the failure-front velocity, which attains the speed of sound. This is accompanied by a decrease in the energy of elastic motion (Fig. 1, curves 5), ensuring a nonuniform decrease in the mass velocity at the perturbation front, as shown by curves 1 in Fig. 3. The upper part of the figure shows the arrival-time dependences of the mass velocity at the front of the main perturbation (curves 1) and of the mass velocity of the precursor (curves 2), and the lower part contains the arrival-time dependences of the peak values of the stresses at the front of both the main perturbation (curves 3) and the precursor (curves 4). Tangential stresses are depicted by crossed lines; they are not shown for the main perturbation front, since in this case they differ little from the radial ones. It is seen that the nature of the dependence of the stress amplitudes on time changes qualitatively with the development of motion. This change is associated not with a change in the failure mechanism, since it occurs earlier, but with the fact that the SWF velocity, which is supersonic in the beginning, becomes equal to the elastic shock wave velocity.

Despite allowance for phase transitions, the state equation used ensures behavior of the shock adiabatic such that an increase in shock-wave loading is accompanied by a monotonous increase in shock-wave velocity. Therefore, in both the present work and [1] phase transition does not ensure shock-wave splitting [4]. When the SWF velocity exceeds the speed of sound, the motion is characterized by an irregular multiwave structure generated by repeated motions of the source, which is also typical of mass explosion in a medium devoid of strength [5]. In such a medium, a regular two-wave structure is brought about by the mechanism of cracking already after the cessation of phase transition and fragmentation. Its incipience and development are shown in Fig. 4, which displays velocity profiles and diagrams of stresses (in the lower parts of the figures) for different time instants. Here again the diagrams of tangential stresses are depicted by crossed lines. Figure 4a corresponds to the time of the incipience of cracks and of a given wave structure, and Fig. 4b corresponds to the time at which the energy content of the crack region is maximal, while Fig. 4c corresponds to the time of stoppage of the cracking front and emergence of the second wave into the elastic region of the first variant. For pure quartz this instant is reached later (see below). It is seen that before the destruction front an elastic wave propagates in which the radial stresses are three times larger than the tangential ones (Fig. 3, curves 4). This region is followed by a zone of open cracks in which tangential stresses relax to zero and radial stresses decrease considerably leading to a rise in the stress curves and dip in the velocity profile shown in Fig. 4b and 4c. This zone is followed by a main wave of large-amplitude stresses, which close the cracks but do not make the medium solid. In this wave different kinds of stresses differ little in magnitude. The change in the energy in the region of cracking is shown in Fig. 1 by curves 4; the trajectories of its boundaries are given in Fig. 2 by curves 5.

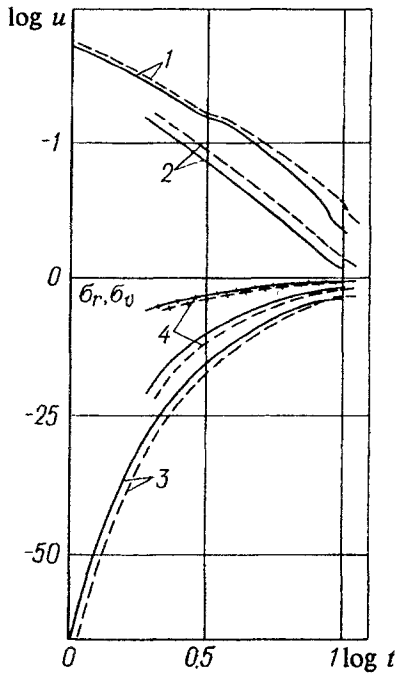

Fig. 3. Dependences of peak values of velocity and stresses on the time of the perturbation wave arrival: 1) mass velocity at the front of the main wave of disturbance; 2) mass velocity of the precursor; 3) amplitude of stresses at the front of main disturbance wave; 4) amplitude of the stresses of the precursor.

These results agree qualitatively with the results presented in [6], where numerical calculation of an explosion in granite is considered. The authors of [6] used the Eulerian representation of the medium and an elastoplastic model of destruction: they also noted the appearance of a two-wave structure during the formation of radial cracks in the process of shock-wave loading.

Thereafter, when the loadings are decreased appreciably, the boundary of the crack region slows down, failure ceases, the energy of the region decreases (Fig. 1, curves 4), and the energy of elastic motion increases again (Fig. 2, curves 5). Then, all kinds of energy are stabilized. Motion in the vicinity of the source continues, as does the emission of elastic energy. Calculations show that most of the original energy of an explosion is spent in phase transformations and failure. The fraction of elastic energy is 8% of the original one. However, despite such smallness, the numerical calculations do not correspond to solutions obtained in acoustic approximations [7, 8]. In those works, elastic energy is emitted in the form of a system of two elastic shock waves in which the peaks of mass velocity and of all kinds of stresses coincide in space.

The emergence of the second elastic wave is accompanied by a decrease in the mass velocity amplitude at its front (Fig. 3, curves 1), by an increase in the amplitude of radial stress (Fig. 3, curves 3), as well as by the establishment in it of the same relationship between the peak values of σ_r and σ_ϑ as in the precursor wave. This relationship is in line with [9, 10], where analytical solutions are given for the problem of an elastic shock wave generated by pressure in a cavity. The double-humped peak of the radial stresses of the second wave in Fig. 4c was formed under the action of a source-induced secondary pulse that ensured the secondary involvement of the processes of cracking responsible for the difference in the σ_r and σ_ϑ profiles. Analysis of the results of numerical calculations made it possible to obtain an approximate equation that relates the distance between the first and second elastic waves to the failure parameters:

$$\lambda = (R_r - R_s)\,(5\sigma_k/\sigma_*)^{1/2}/(1 - (5\sigma_k/\sigma_*)^{1/2})\,. \tag{2}$$

Here R_r is the radius of the crack region, R_s is the radius of the fragmentation region, and σ_* is the stress acting on the boundary of the region of cracks. In the case of phase transition, the value of λ is by 14.8% smaller than that for pure quartz.

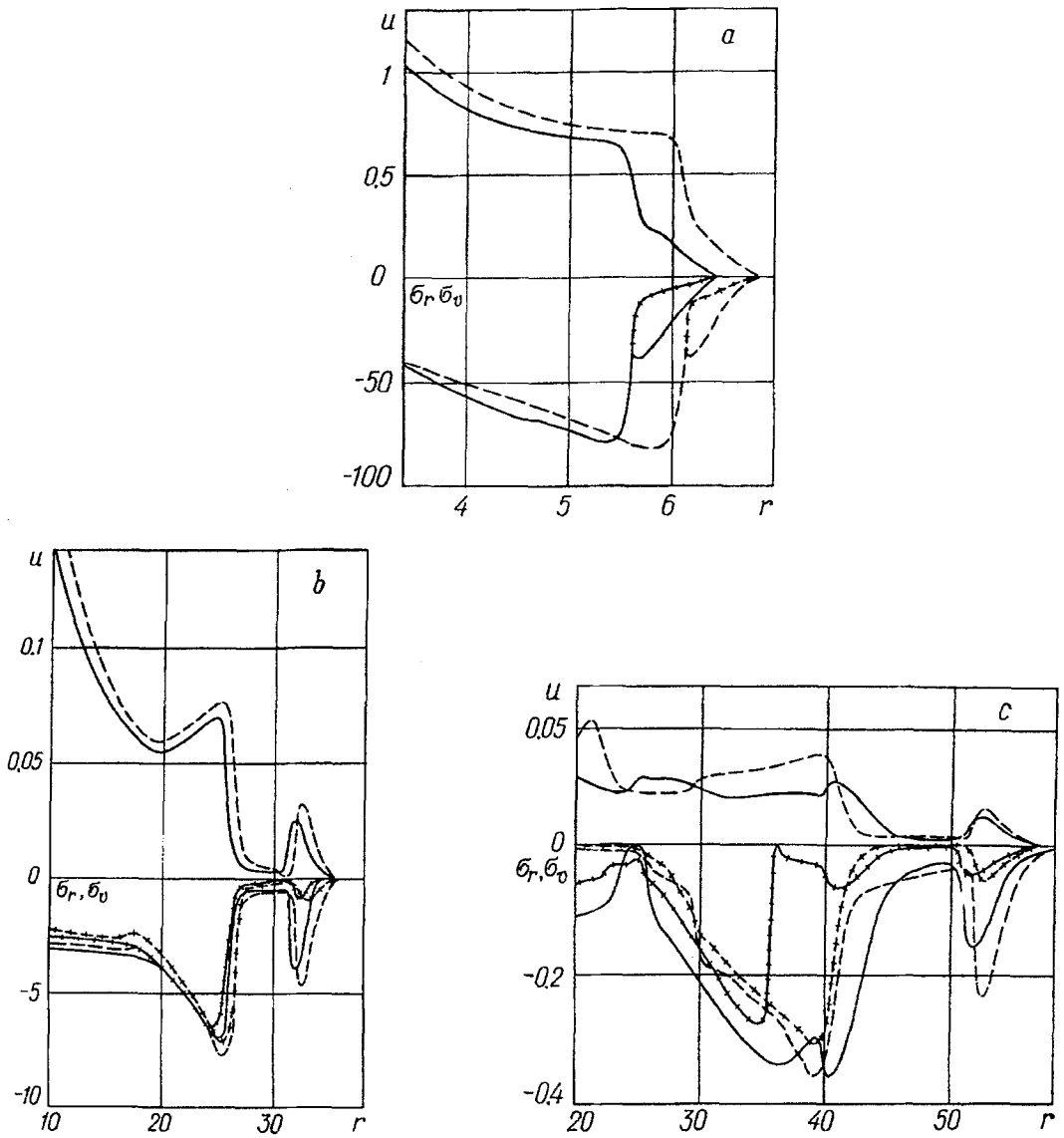

Fig. 4. Velocity profiles and diagrams of stresses for three time moments: a) beginning of the period of the formation of cracks; b) middle of the period; c) stoppage of the front of cracking.

The emission of the second elastic wave is accompanied by the establishment of peak stresses σ_r and σ_ϑ, whose amplitudes differ little; the peak is associated with an immobile boundary of the region of cracks and is in accord with the maximum of pressure and density. The amplitudes of the mass velocity and radial stress correspond to the second wave. The front of the third peak is followed by an irregular multiwave structure of motion directed from the center. When this motion is weakened sufficiently, an opposite motion directed to the center is formed, during the development of which split-off failure can occur, since the medium is sufficiently loaded. This assumption is made on the basis of observations [11] according to which the explosion cavity always caves-in in brittle rocks, with the dimensions of caving always exceeding the radius of the cracks region. Apparently, these failure also generate elastic waves whose amplitudes are smaller than the amplitudes of the first two waves.

It is to be expected that the process of the split-off failure completes the formation of an acoustic emitter generated by an explosion. Using the results obtained and the uncertainty principle [12], according to which the width of the spectrum of the ΔH signal and its duration $\Delta\tau$ are connected by the relation $\Delta H \Delta\tau$ = const, we can estimate the effect of processes in the near and middle explosion zones on the spectrum of acoustic emission. In this case the duration of the signal is $\Delta\tau \sim R_x$ (R_x is the radius of the emitter equal to the radius of the region of split-off cracks), since internal motions of the emitter, not having extraneous sources, are transformed into

emission. From this it is clear that phase transitions ensure broadening of the spectrum, as they lead to a decrease in the radius of the failure region (see Fig. 2). Providing a considerable growth of the failure region and the dimensions of the emitter, cracking processes lead to narrowing of the spectrum. Evidently, these processes determine the detailed structure of the acoustic emission spectrum. Thus, in the absence of either phase transitions or cracking, the emission will have a spectrum of wide-range noise. In this case the spectral density has a maximum at the low-frequency boundary of the emission band and decreases with an increase in frequency. Taking account of the fact that in our case the second elastic peak exceeds the remaining ones, we, proceeding from the results of [12], can assume that this maximum corresponds to the frequency $f = C_l/\lambda$, where C_l is the longitudinal speed of sound, and that it is located near the band center. (Here, it is taken into account that in the case of a confined explosion a signal, whose frequency is determined by C_l, can propagate in air after emergence from the day surface.) If we avail ourselves of the relationship between R_r and R_s suggested in [11], we can easily obtain the estimate $f \sim R^{1/2}$, which is of interest for experimental verification. The same estimate is obtained for the width of the spectrum. Here P is the hydrostatic pressure, which in our case is equal to zero. If there are both cracking and a phase transition that ensures splitting of the shock wave, then, since cracking leads to additional shock-wave splitting, the spectral density at the center of the band will have several peaks with close values of the maxima. However, we failed to check this by numerical experiment. We had to interrupt calculation even before the stage of splitt-off failure, because the equation of state suggested in [1] was quite satisfactory in the near and middle explosion zones, but turned out to be unsatisfactory in the elastic region at small degrees of compression at loadings smaller than σ_0. Under such conditions it leads to nonphysical values of pressure and needs modification.

As seen from the figures, there is no qualitative difference between the results of calculations by the two variants, despite the qualitative difference between the equations of state used in them. Quantitative differences arise from allowance for the quartz-stishovite phase transformation. Figure 1 shows that phase transition virtually does not influence the process of energy transfer from the source to the surrounding medium but exerts a substantial influence on the transfer of energy in it. It is seen that the energy content of the melt in the presence of stishovite greatly exceeds that for pure quartz. At the same time, the relationship between the energy contents in the region of fragmentation is reversed. This is explained by the fact that the main mass of the stishovite formed is contained in the melt, and also by large energy expenditures for this transformation. Stishovite is a highly dense phase, the speed of sound in which is two times larger than in quartz, affording this rock good accumulating properties. This ensures an effective increase in the strength of a medium that undergoes such a transition: smaller peak values of stresses and mass velocity in each fixed time instant, earlier appearance of the elastic precursor and cessation of destruction, and smaller failure regions as compared with the case of pure quartz. For the first variant, the thicknesses of the layers of melt, crushed rock, and cracks are, respectively, smaller by 102.7%, 36.7%, and 10% than the values for the second variant, while the dimensions of the cavities of explosion coincide.

Comparison of the results of the present work (obtained for the first variant and corresponding to the near zone of explosion) with the results presented in [1] reveals qualitative agreement of the time dependence of the amplitude of pressure and velocity profiles. However, we did not obtain the intersection of velocity profiles shown in [1]. The difference is explained by energy expenditures for fragmentation, which was taken into consideration in our calculation and decreased the velocity profiles for comparable times.

The foregoing permits us to make the following conclusions.

1. The use of hydrodynamic approximation for calculating unsteady motions of a strong medium is admissible only in the near zone of explosion, when the SWF velocity exceeds the speed of sound where melting occurs. In the case of fragmentation, it permits one to obtain only rough estimates of the SWF parameters.

2. Calculation of motions in the near zone, if the medium in it undergoes cracking, or in the middle zone, when the SWF velocity becomes equal to the speed of sound and an elastic precursor is formed, requires that the strength properties of the medium and the mechanisms of its destruction be fully taken into account.

3. In contrast to phase transitions, the processes of cracking always lead to shock-wave splitting. Therefore, a regular two-wave structure of shock-wave elastic motion can be connected with phase transition only under conditions that prevent the formation of cracks, namely either in the case of corresponding hydrostatic loading [11] or when the breaking strength is higher than the strength of compression.

4. When cracking is present and phase transition ensures shock-wave splitting, one should expect the appearance of a richer regular wave structure.

5. The structure of the shock-wave elastic motion generated by an explosion in a solid medium contains essential information about the processes occurring in the near and middle zone of explosion: specific features of phase transitions, forms and specific features of failure, and the dimensions of failed regions.

6. The effect of processes occurring in the near and middle zones of an explosion on the characteristics of acoustic emission generated by it is unambiguous. Phase transitions ensure broadening, while cracking processes cause narrowing of the emission band. The effect of these processes on the detailed structure of the acoustic spectrum requires further investigation.

7. The state equation suggested in [1] is applicable for describing the behavior of a substance in a wide range of shock-wave loading. However, for loading smaller than 10^8 Pa it gives nonphysical values of pressure and needs modification.

NOTATION

γ, specific heat ratio of a perfect gas; t, dimensionless time; t_0, unit time; ρ_0, unit density; r, dimensionless distance; R_0, unit of distance; u, dimensionless velocity; C_0, unit velocity; Y, elastic limit; S_i, components of stresses deviator; σ_k, ultimate breaking strength; σ_r, dimensionless radial stress; σ_ϑ, dimensionless tangential stress; σ_0, unit stress; E_0, energy of the source of explosion; λ, spacing between elastic shock waves; R_s, radius of fragmentation region; R_r, radius of crack region; σ_*, stress acting at the boundary between crack region and region of elastic motion; f, frequency corresponding to the maximum of the spectral density of acoustic signal; C_l, longitudinal speed of sound; P, hydrostatic pressure; ΔH, width of the spectrum of acoustic emission; $\Delta\tau$, duration of acoustic signal; R_x, radius of an acoustic emitter generated by explosion.

REFERENCES

1. S. S. Grigoryan, L. S. Evterev, E. V. Zamyshlyaev, and S. G. Krivosheev, Dokl. Akad. Nauk SSSR, **241**, No. 6, 1292-1295 (1978).
2. V. A. Bychenkov, V.V. Gadzhieva, and V. F. Kuropatenko, Chisl. Metody Mekh. Splosh. Sred, **3**, No. 2, 3-17 (1972).
3. A. M. Petrenko, "Solution of one-dimensional problems of gas dynamics and mechanics of solid and destructible medium. Algorithms and programs," Informats. Byullet., No. 11, 4 (1988).
4. Ya. B. Zel'dovich and Yu. P. Raizer, Physics of Shock Waves and High-Temperature Hydrodynamic Phenomena [in Russian], Moscow (1966).
5. G. Brode, News in Foreign Science, No. 4 [in Russian], Moscow (1976).
6. E. Fachioli and H. S. Ang, in: The Action of a Nuclear Explosion [Russian translation], Moscow (1971), pp. 163-253.
7. E. Skuchik, Foundations of Acoustics, Vol. 2 [in Russian], Moscow (1976).
8. M. A. Isakovich, General Acoustics [in Russian], Moscow (1973).
9. G. Hopkins, Dynamic Inelastic Deformations of Metals [in Russian], Moscow (1964).
10. Mechanical Effect of an Underground Explosion [in Russian], Moscow (1971).
11. V. N. Rodionov, I. A. Sizov, and A. M. Tsvetkov, Foundations of Geomechanics [in Russian], Moscow (1986).
12. J. Bendat, Foundations of the Theory of Random Noise and Its Application [Russian translation], Moscow (1965).